LETTER

doi:10.1038/nature11287

A restricted cell population propagates glioblastoma growth after chemotherapy

Jian Chen[1], Yanjiao Li[1], Tzong-Shiue Yu[1,2]†, Renée M. McKay[1], Dennis K. Burns[3], Steven G. Kernie[1,2]† & Luis F. Parada[1]

Glioblastoma multiforme is the most common primary malignant brain tumour, with a median survival of about one year[1]. This poor prognosis is due to therapeutic resistance and tumour recurrence after surgical removal. Precisely how recurrence occurs is unknown. Using a genetically engineered mouse model of glioma, here we identify a subset of endogenous tumour cells that are the source of new tumour cells after the drug temozolomide (TMZ) is administered to transiently arrest tumour growth. A *nestin-ΔTK-IRES-GFP* (*Nes-ΔTK-GFP*) transgene that labels quiescent subventricular zone adult neural stem cells also labels a subset of endogenous glioma tumour cells. On arrest of tumour cell proliferation with TMZ, pulse-chase experiments demonstrate a tumour re-growth cell hierarchy originating with the *Nes-ΔTK-GFP* transgene subpopulation. Ablation of the GFP$^+$ cells with chronic ganciclovir administration significantly arrested tumour growth, and combined TMZ and ganciclovir treatment impeded tumour development. Thus, a relatively quiescent subset of endogenous glioma cells, with properties similar to those proposed for cancer stem cells, is responsible for sustaining long-term tumour growth through the production of transient populations of highly proliferative cells.

We have extensively studied a series of mouse strains harbouring conditional alleles of the tumour suppressors *Nf1*, *p53* (also known as *Trp53*) and *Pten*, which spontaneously develop malignant gliomas with 100% penetrance, and have identified the source cells of these tumours as deriving from the subventricular zone (SVZ)[2–4]. Thus, we proposed that adult neural stem cells (NSCs) are the likely source of these tumours[2]. We wished to determine whether a *Nes-ΔTK-GFP* transgene[5], originally devised to mark adult NSCs, would also mark endogenous glioma cells. Elements of the nestin gene can drive transgene expression specifically in adult NSCs[2,5] (Fig. 1a). The transgene also harbours a cassette containing a modified version of the herpes simplex virus (HSV) thymidine kinase (ΔTK), allowing for temporally regulated ablation of dividing neural progenitors by systemic ganciclovir (GCV) administration, and an IRES-GFP cassette to mark *Nes-ΔTK*-expressing cells in the absence of GCV. The *Nes-ΔTK-GFP* transgenic mice showed the expected expression in both glial fibrillary acidic protein (GFAP)-positive adult NSCs and early doublecortin (DCX)-positive neural progenitor cells (NPCs) in the major adult NSC niche: the SVZ of the lateral ventricle (Fig. 1b, c). To validate that the GCV-activated *Nes-ΔTK-GFP* transgene could effectively eliminate endogenous neural stem/progenitor cells, 1-month-old transgenic mice were treated with GCV for 2 weeks. In control mice, the rostral migratory stream (RMS), formed by NPCs migrating from the SVZ to the olfactory bulb, is visualized by Nissl staining. In contrast, the RMS was severely diminished in *Nes-ΔTK-GFP* mice after GCV treatment (Fig. 1b, bottom). Consistent with this observation, DCX immunostaining indicated the absence of NPCs in the SVZ of GCV-treated *Nes-ΔTK-GFP* animals (Fig. 1c, bottom). Because, in the presence of GCV, HSV TK targets only proliferating cells, the GFAP$^+$ NSCs that remained quiescent were unaffected, although they also express the transgene, as indicated by GFP (Fig. 1c, bottom). Thus, our *Nes-ΔTK-GFP* transgene is specifically expressed in SVZ quiescent

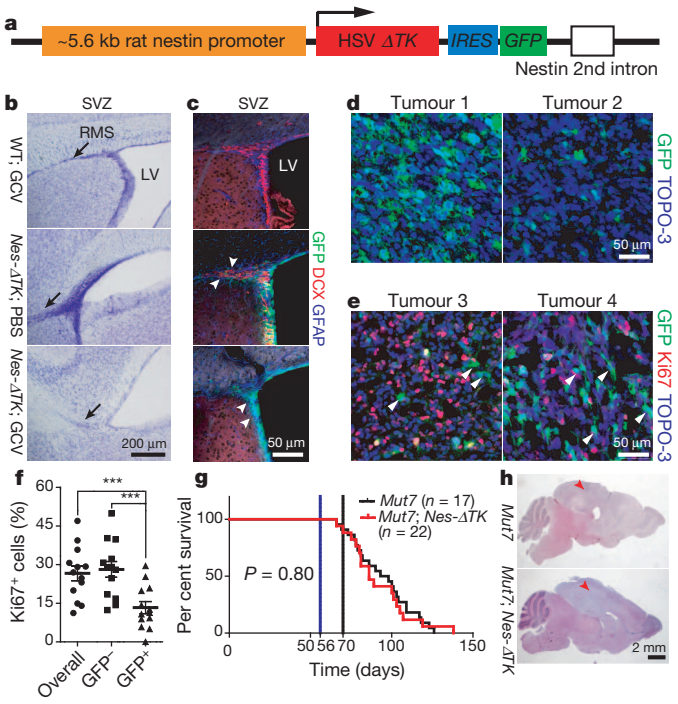

Figure 1 | Characterization of the *Nes-ΔTK-GFP* transgene. **a**, Diagram of the *Nes-ΔTK-GFP* transgene. **b**, **c**, GCV administration ablates NSCs in wild-type mice. **b**, Representative Nissl staining of the SVZ region in wild-type mice treated with GCV (WT; GCV), *Nes-ΔTK* transgenic mice treated with PBS (*Nes-ΔTK*; PBS) and *Nes-ΔTK* transgenic mice treated with GCV (*Nes-ΔTK*; GCV); black arrows indicate the stem cell RMS, which is greatly reduced in *Nes-ΔTK* mice treated with GCV. **c**, GFP (transgene), GFAP (quiescent NSCs) and DCX (committed neural progenitors) immunostaining of the SVZ stem cell niche. White arrowheads in middle panel (*Nes-ΔTK*; PBS) indicate DCX$^+$ GFP$^-$ cells more distal in the RMS. White arrowheads in bottom panel (*Nes-ΔTK*; GCV) indicate GFP$^+$/GFAP$^+$ but DCX$^-$ quiescent NSCs. **d**, Representative GFP immunostaining in sections from two untreated gliomas of *Mut7;Nes-ΔTK* mice. From tumour to tumour, varying numbers of GFP$^+$ cells were observed. TOPO-3 stains nuclei. **e**, Representative GFP and Ki67 co-immunostaining in two untreated gliomas of *Mut7;Nes-ΔTK* mice. White arrowheads highlight GFP$^+$ but Ki67$^-$ cells, demonstrating that many transgene GFP$^+$ cells are quiescent. **f**, Percentage of Ki67$^+$ cells in GFP$^+$, GFP$^-$, and overall tumour population in gliomas from untreated *Mut7;Nes-ΔTK-GFP* mice. **g**, Kaplan–Meier survival curve of untreated *Mut7* and *Mut7;Nes-ΔTK* animals. No difference in per cent survival was observed. **h**, Representative haematoxylin and eosin staining of *Mut7* and *Mut7;Nes-ΔTK* brains without treatment. Infiltrative malignant gliomas are present in the cortex (red arrowhead) of both genotypes. ***$P < 0.001$.

[1]Department of Developmental Biology & Kent Waldrep Center for Basic Research on Nerve Growth and Regeneration, University of Texas Southwestern Medical Center, Dallas, Texas 75390-9133, USA. [2]Department of Pediatrics, University of Texas Southwestern Medical Center, 5323 Harry Hines Boulevard, Dallas, Texas 75390, USA. [3]Department of Pathology, University of Texas Southwestern Medical Center, 5323 Harry Hines Boulevard, Dallas, Texas 75390, USA. †Present address: Department of Pathology and Cell Biology, Columbia University, New York, New York 10032, USA.

and proximal progenitor cells, and chronic GCV administration effectively blocks neurogenesis by ablating quiescent cells as they enter the cell cycle.

We bred the *Nes-ΔTK-GFP* transgene into *hGFAP-Cre;Nf1*$^{fl/+}$;*p53*$^{fl/fl}$;*Pten*$^{fl/+}$ (*Mut7*) glioma-prone mice[3]. *Mut7* mice develop malignant glioma, with full penetrance, by somatic deletion of three of the most frequently mutated tumour suppressors in glioblastoma multiforme: p53, NF1 and Pten[6]. All *Mut7;Nes-ΔTK-GFP* mice also developed gliomas and we observed only a subset of tumour cells expressing GFP (*Nes-ΔTK-GFP* positive; Fig. 1d, e). These cells also co-expressed the neural stem cell marker Sox2 (not shown). We next examined tumour cell proliferation and found that *Mut7;Nes-ΔTK-GFP* tumours exhibited a significant proportion of Ki67$^+$/GFP$^-$ cells, and conversely, the subset of GFP$^+$ tumour cells rarely co-stained for Ki67 (Fig. 1e, f). These data indicate that most transgene GFP$^+$ tumour cells are relatively quiescent in comparison to a highly proliferative (Ki67$^+$) subpopulation reminiscent of the SVZ, where GFP$^+$ stem cells are quiescent compared to GFP$^-$ progenitors (Fig. 1c). Furthermore, as in wild-type mice, in which the *Nes-ΔTK-GFP* transgene does not affect SVZ neurogenesis in the absence of GCV administration (Fig. 1b, c), introduction of the transgene into the *Mut7* genetic background did not affect tumour development or enhance survival (Fig. 1g). Like *Mut7* mice, *Mut7;Nes-ΔTK-GFP* mice developed malignant glioma with 100% penetrance and with similar kinetics (Fig. 1g, h).

TMZ is a DNA alkylating agent that is currently the primary chemotherapy administered to glioblastoma multiforme patients[7] as it has transient tumour growth-arrest properties. We found that TMZ eradicates proliferative cells in the endogenous murine gliomas. TMZ was administered over several days to tumour-bearing mice followed by BrdU injection 2 hours after final treatment, and the mice were killed 2 hours thereafter (Fig. 2a). The TMZ-treated mice showed a marked reduction of BrdU incorporation in both tumours and NSC niches (Fig. 2b, c). Similar to treated glioma patients after TMZ treatment, the murine tumours reinitiated cell division and growth. Thus, TMZ targets proliferating cells but tumour recurrence is inevitable. To examine the details of tumour recurrence, we traced the first wave of tumour cell proliferation after completion of the drug regimen in tumour-bearing mice by pulse chase using the BrdU analogues CldU and IdU. CldU and IdU were injected 1 day and 3 days, respectively, after the final TMZ injection (Fig. 2d). Given the variable but relatively low proportion of GFP$^+$ cells in all tumours (Fig. 1d, e), we reasoned that if cell proliferation reinitiated randomly in tumour cells after TMZ treatment, then the number of GFP$^+$ cells that would incorporate CldU and/or IdU should be low to insignificant. However, if renewed tumour cell proliferation was hierarchical and derived from the GFP$^+$ cells, a biased incorporation of nucleotide analogues into the relatively small GFP$^+$ cohort of tumour cells would result. Examination of tumour sections with immunohistochemistry revealed that the large majority of cells incorporating CldU and IdU after relatively short chases also contained GFP expression (Fig. 2e; GFP percentage in CldU$^+$ population = 77 ± 14, GFP percentage in IdU$^+$ population = 83 ± 10). Moreover, IdU$^+$ cells retained both GFP and CldU, indicating that after TMZ eradication of a majority of pre-existing proliferating tumour cells, the re-emergent population of proliferating cells derived from *Nes-ΔTK-GFP*-expressing cells and not from random tumour or other specific subsets of cells (Fig. 2e; CldU percentage in IdU$^+$ population = 86 ± 9). When the second, IdU, pulse was prolonged to a 7-day chase after the CldU pulse, most IdU cells double-labelled for CldU (85 ± 7%) but lost GFP expression (Supplementary Fig. 1a–c). Thus, as in the normal SVZ stem cell niche, over time the GFP-expressing glioma cell population gives rise to cells that progressively lose stem cell properties (that is, nestin expression and relative quiescence) and concomitantly shut down the *Nes-ΔTK-GFP* transgene (Supplementary Fig. 1c, d). Using endogenous lineage tracing of renewed cell division within tumours, we have identified the

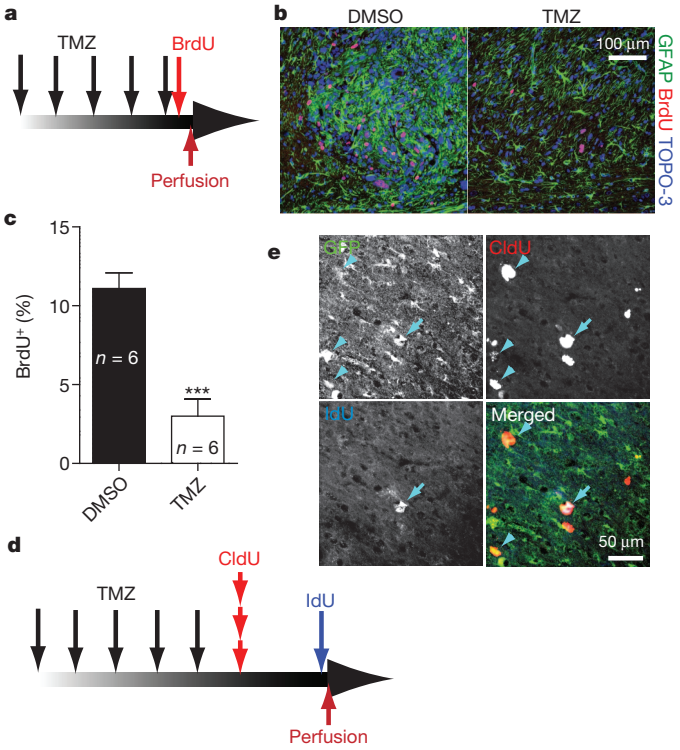

Figure 2 | TMZ targets proliferating derivatives but not the GFP$^+$ quiescent cell population. **a**, TMZ injection schema. *Mut7* mice were treated with TMZ for 5 days, injected with BrdU 2 h after the final TMZ treatment, and killed 2 h later for BrdU immunostaining. **b**, Representative GFAP/BrdU co-staining of glioma from DMSO- or TMZ-treated mice shows a marked reduction in the number of BrdU$^+$ cells. **c**, Quantification of the percentage of maximal BrdU$^+$ cells in gliomas from *Mut7* mice treated with or without TMZ showed a significant decrease in the TMZ-treated mice. Data are mean ± s.e.m.; $n = 6$ for each treatment; $^{***}P < 0.001$, Student's *t*-test. **d**, **e**, *Nes-ΔTK*$^+$ cells are resistant to TMZ and produce new tumour cells. **d**, Schema of TMZ treatment and short-term labelling with BrdU analogues. *Mut7;Nes-ΔTK* mice were treated with TMZ for 5 days and then injected with the BrdU analogues CldU and IdU 1 and 3 days after the last TMZ treatment, respectively. **e**, Representative tumour section illustrating that repopulating tumour cells after TMZ treatment express the *Nes-ΔTK* transgene (GFP$^+$); merged panel, CldU-incorporating (arrowhead) or IdU-incorporating (arrow) cells also express GFP driven by the *Nes-ΔTK* transgene. (Percentage of GFP$^+$ cells in the CldU$^+$ population = 77 ± 14; percentage of GFP$^+$ cells in the IdU$^+$ population = 83 ± 10; $n = 5$.) Note that the majority of CldU$^+$ cells and IdU$^+$ cells are positive for GFP expression, and also that the majority of IdU$^+$ cells are CldU$^+$, indicating that the CldU$^+$ cells gave rise to the IdU$^+$ cells.

relatively quiescent *Nes-ΔTK-GFP*-expressing tumour cells as the primary source of proliferating and eventually non-dividing tumour cell derivatives (Supplementary Fig. 1c, d). In addition, the data show that in our endogenous glioma models, TMZ targets the proliferating derivatives but not the GFP$^+$ quiescent cells.

One prediction would be that eradication of the GFP$^+$ cells in the endogenous tumours should considerably decrease the emergence of new dividing tumour cells. We tested this prediction at two stages: early endogenous tumour development and advanced tumour development. First, *Mut7;Nes-ΔTK-GFP* mice were treated with GCV beginning at 8 weeks of age—the earliest time of detectable pre-tumorigenic anomalies[3]. To capture most quiescent GFP$^+$ cells in a dividing state, GCV treatment lasted for 10 weeks, requiring three osmotic mini-pump placement surgeries that unfortunately were accompanied by complications, resulting in considerable variance of drug delivery. Drug-delivery efficacy was qualitatively measured by examination of the normal stem cell niche response to drug (Fig. 1b, c) as manifested by residual RMS (Supplementary Fig. 2a). Accordingly, tumour incidence varied from mouse to mouse, with some perishing

early with large tumours. However, as a group, the GCV-treated cohort showed a clear survival advantage (Fig. 3a). After 10 weeks of treatment, the only surviving mice were among those treated with GCV (Supplementary Fig. 2b), and analysis of their brains revealed only low-grade lesions (Supplementary Fig. 2c). When GCV was effectively delivered, survival was substantially prolonged and tumour progression was severely impaired. Thus, elimination of *Nes-ΔTK-GFP*$^+$ cells at early/pre-tumorigenic stages prevents development of high-grade gliomas.

A second GCV regimen was started in 10-week-old tumour-bearing mice. Most 10-week-old *Mut7* mice do not show neurological symptoms, yet histological examination of large cohorts showed that all mice harbour astrocytomas of differing grades (Supplementary Fig. 3). We subjected 10-week-old *Mut7;Nes-ΔTK-GFP* or *Mut7* mice to GCV or saline for 2 months. GCV treatment of *Mut7;Nes-ΔTK-GFP* mice improved survival by approximately 30 days compared to saline control, whereas neither treatment was effective in improving survival of *Mut7* mice (Fig. 3b). Consistent with this, GFP and endogenous nestin double immunostaining showed that GFP$^+$ cells were successfully eliminated in gliomas of *Mut7;Nes-ΔTK-GFP* mice after prolonged GCV treatment (Fig. 3c).

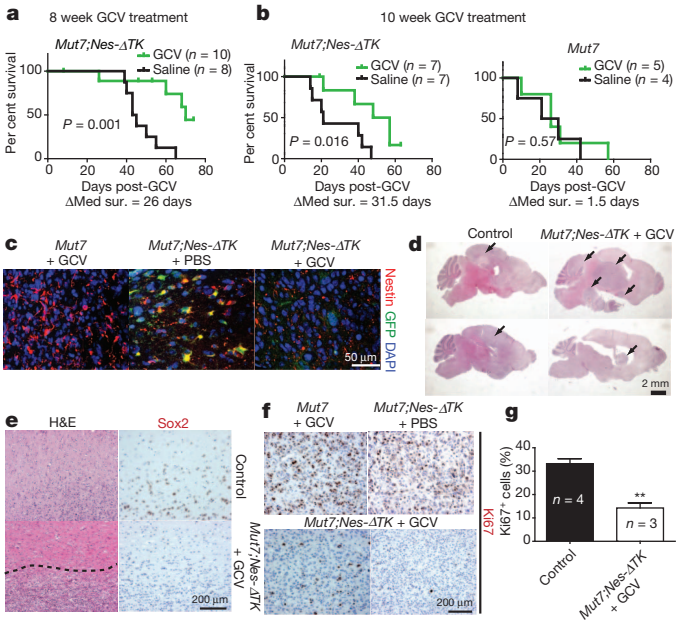

Figure 3 | GCV treatment prolongs survival of *Mut7;Nes-ΔTK* mice. **a**, Kaplan–Meier curve of *Mut7;Nes-ΔTK* mice treated with saline or GCV for 10 weeks starting at 8 weeks of age showed a clear survival advantage for the GCV-treated mice ($n = 10$ for GCV-treated; $n = 8$ for saline-treated; P values determined using log-rank test). ΔMed sur., change in median survival. **b**, Kaplan–Meier survival curves of *Mut7;Nes-ΔTK* (left) or *Mut7* (right) mice treated with GCV or saline for 2 months starting at 10 weeks of age. GCV treatment increased survival of *Mut7;Nes-ΔTK* mice compared to saline treatment but had no such effect on the *Mut7* mice. $n = 5$–7 for the GCV-treated mice; $n = 4$–7 for the saline-treated mice; P values determined using log-rank test. **c**, GFP/nestin co-immunostaining of gliomas from control (*Mut7* mice treated with GCV or *Mut7;Nes-ΔTK* mice treated with PBS) and GCV-treated *Mut7;Nes-ΔTK* mice. Elimination of GFP and nestin double-positive cells in the *Mut7;Nes-ΔTK* mice treated with GCV from 10 weeks. **d**, Representative haematoxylin and eosin staining of control and GCV-treated *Mut7;Nes-ΔTK* brains. The tumours in the GCV-treated *Mut7;Nes-ΔTK* mice are less infiltrative than in control. Tumours are indicated by black arrows. **e**, Representative haematoxylin and eosin (H&E) and Sox2 staining of tumour edges in control and GCV-treated *Mut7;Nes-ΔTK* tumours showing the GCV-treated tumours have a defined boundary (dotted line) and lack infiltrative Sox2$^+$ cells. **f**, **g**, GCV treatment decreases proliferation index in *Mut7;Nes-ΔTK* tumours. **f**, Representative Ki67 staining of control (top) or GCV-treated *Mut7;Nes-ΔTK* tumours (bottom) showing the marked decrease in proliferation in the GCV-treated *Mut7;Nes-ΔTK* tumours. **g**, Quantification of the percentage of Ki67$^+$ cells in tumour regions with highest number of proliferating cells in cortex. The percentage is significantly decreased in GCV-treated *Mut7;Nes-ΔTK* mice ($n = 3$) versus control ($n = 4$). Data are mean ± s.e.m.; $^{**}P < 0.01$, Student's t-test.

The residual tumours in these tumour-bearing *Mut7;Nes-ΔTK* mice treated with GCV beginning at 10 weeks of age did not have the classic glioma feature of invasiveness but instead were circumscribed with well-defined boundaries (Fig. 3d, e and Supplementary Fig. 2d, e). Although the *Mut7;Nes-ΔTK-GFP* transgene is only expressed in a subset of cells in the untreated tumour (Fig. 1e), tumours in GCV-treated *Mut7;Nes-ΔTK* mice showed a marked reduction of Ki67$^+$ cells and stem cell markers (Fig. 3e–g). These data further support the hypothesis that chronic GCV administration progressively ablates the relatively quiescent GFP$^+$ tumour cell population and the remaining GFP$^-$ tumour cells eventually exhaust their proliferative and infiltrative potential.

The HSV TK system has been widely used as a method to induce endogenous cell suicide. A potentially confounding phenomenon is the 'bystander effect', whereby HSV-TK-expressing cells not only commit suicide in the presence of GCV, but can also induce the death of neighbouring non-TK-expressing cells[6]. However, several NSC-specific HSV-TK-expressing transgenic mice have been reported and no bystander effect has been described[8–11]. To examine whether tumour development was appreciably impaired by the bystander effect, we turned to transplantation assays.

We first determined whether GCV treatment would also blunt *Mut7;Nes-ΔTK-GFP* tumour growth in a transplantation assay. Primary gliomas from *Mut7;Nes-ΔTK-GFP* and *Mut7* mice were dissociated and directly injected subcutaneously into nude mice in the presence of continuous GCV or saline treatment (Supplementary Fig. 4a). Neither GCV nor saline affected the tumour growth of *Mut7*-derived cells (Supplementary Fig. 4b). In contrast, similar to a previous report[12], mice transplanted with *Mut7;Nes-ΔTK* tumour cells and then treated with GCV developed significantly smaller tumours that appeared to be poorly vascularized compared to saline-treated controls (Supplementary Fig. 4c–f). Thus, the *Mut7* tumour cells transplant efficiently in immunocompromised mice and, as in the endogenous setting (Fig. 3), GCV treatment severely impairs tumour development after transplantation. To test for the bystander effect, we transduced primary *Mut7* cells with a lentivirus harbouring either a control RFP cassette or an HSV TK cassette (Supplementary Fig. 5a). Mixed ratios of the two cell populations were injected subcutaneously into nude mice and allowed to seed tumours for 4 weeks, after which GCV was administered for 2 weeks (Supplementary Fig. 5b). The data indicate that the presence of a 10%, 20% or 50% initial ratio of TK-expressing tumour cells did not impair tumour development of the non-TK-expressing cells in the presence of GCV (Supplementary Fig. 5c, d). In the extreme case when equal numbers of TK$^+$ (10^5) and TK$^-$ (10^5) cells were injected compared to 10^5 TK$^-$ cells alone, tumour development was equivalent in both cohorts, demonstrating that GCV toxicity to 50% of the tumour cells did not extend into the TK$^-$ tumour cell population (Supplementary Fig. 5c, d). In our endogenous tumours, such a bystander effect would require the relatively rare GFP$^+$ tumour-propagating cells to be widely toxic in order to have a considerable paracrine effect on tumour properties. Instead, these studies indicate that GCV administration does not have an appreciable effect on cells outside those expressing the *TK* gene, consistent with other recently reported studies[8–12]. We conclude that eradication of the *Mut7;Nes-ΔTK-GFP* endogenous tumour cells through GCV treatment effectively disrupts the continued production of tumour cells, as predicted from the preceding data.

Despite effective depletion of GFP-expressing tumour-propagating cells with GCV treatment, a considerable residual tumour mass remained (Fig. 3d). We therefore attempted a therapeutic strategy to eliminate both the rapidly proliferating tumour cells and the quiescent

GFP$^+$ cells by sequentially administering TMZ and GCV (TMZ/GCV), respectively (Fig. 4a, b). Initially it seemed that this regimen did not prolong survival beyond that of GCV treatment alone (Fig. 4c). However, examination of the brains of the sequentially treated mice revealed only vestigial tumours in the dorsal brain that showed no transgene GFP expression, indicating effective depletion (Fig. 4d). The cellular density of the residual TMZ/GCV-treated tumours was lower than that of tumours at the beginning of treatment (10 weeks), indicating a statistically significant reduction in tumour bulk. This contrast was markedly enhanced when treated tumours were compared to untreated control tumours (Fig. 4e), which manifested in a spectrum of survival time from 12–16 weeks. Thus, the combined treatment had dramatic inhibitory effects on dorsal tumour growth in these mice.

We were puzzled that TMZ/GCV treatment did not significantly prolong survival beyond the GCV-only treated mice, in which residual circumscribed tumour mass remained (Fig. 3d, e and Supplementary Fig. 2d, e). Analysis of the TMZ/GCV-treated brains revealed that, despite the marked inhibition of original tumour growth, these mice developed novel tumours in the ventral brain region. Six out of seven TMZ/GCV-treated mice had tumours in the brainstem region, whereas gliomas in untreated *Mut7* mice and their remnants in the successfully treated mice are predominantly located in the dorsal/midbrain (Supplementary Fig. 6a). Examination of the TMZ/GCV-resistant hindbrain tumours revealed high endogenous nestin protein but no GFP expression (Supplementary Fig. 6b, c). We also searched archived material and found that a small percentage of *Mut7* brains harboured both dorsal and ventral tumours that we now appreciate were independently arising and not extensions of the dorsal tumours. Appearance of ventral tumours in the presence of GCV indicates an inactive *Nes-ΔTK-GFP* transgene, and direct examination of untreated *Mut7;Nes-ΔTK-GFP* mice demonstrated that the *Nes-ΔTK-GFP* transgene was indeed silent (Supplementary Fig. 6b, e).

We next examined the expression of tumour markers in these hindbrain tumours. In contrast to typical *Mut7* or *Mut7;Nes-ΔTK-GFP* gliomas, all ventral tumours in the TMZ/GCV group showed low levels of endogenous GFAP but relatively high levels of S100B (Supplementary Fig. 6c and data not shown). Seven out of eleven tumours in the ventral and brain stem region of GCV-treated mice (GCV alone or TMZ and GCV) showed histopathological features of oligodendroglioma (Supplementary Fig. 7a–c), including high PDGFR-α levels (Supplementary Fig. 7d). This is in contrast to the pure astrocytic tumours typically observed in this mouse model in the absence of TMZ/GCV. Thus, these data indicate that the ventral tumours that become evident after TMZ/GCV treatment are oligoastrocytic, independently arising, and distinct from the dorsal tumours. Such tumours were recently described in *Mut3* mice[13], and the source was reported to be oligodendroglial progenitors. We are currently further characterizing these tumours.

Our *Nes-ΔTK-GFP* transgene labels SVZ stem cells and, fortuitously, a specific subset of glioblastoma multiforme cells that possesses many features proposed for cancer stem cells (CSCs). The CSC hypothesis holds that some tumours are composed of a hierarchical cadre of cells of which only a subset retains both self-renewal and differentiation capacity[14]. In this model, only CSCs have the capacity to sustain tumour growth and are responsible for recurrence after therapy fails.

The current standard for evaluating whether solid tumours contain CSCs is an *ex vivo* limiting dilution tumorigenic transplantation assay into immunodeficient animals[14]. However, controversy regarding the presence and frequency of solid tumour CSCs remains, probably as a reflection of the variability that accompanies such assays[15–18]. Our study identifies a putative endogenous glioma stem cell located at the apex of a cellular hierarchy in tumour maintenance and recurrence after chemotherapy (Fig. 4a). Continued evaluation of these cells and their properties, including isolation and genetic lineage tracing, may yield important insights into novel therapeutic targets for this intractable disease.

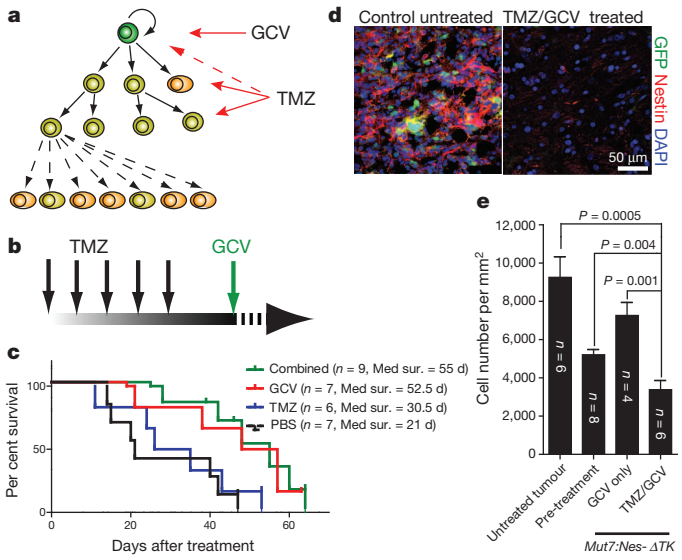

Figure 4 | Combination treatment of TMZ and GCV inhibits glioma progression in cerebrum. **a**, **b**, Therapeutic schema targeting both CSCs and their proliferating progeny. *Mut7;Nes-ΔTK* mice were treated with TMZ for 5 days, followed 2 days after by GCV. **c**, Kaplan–Meier survival curve of *Mut7;Nes-ΔTK* mice with different treatments. GCV-treated ($n = 7$; median survival (Med sur.) = 55 days) and TMZ/GCV-treated ($n = 9$; median survival = 52.5 days) *Mut7;Nes-ΔTK* mice had a similar survival advantage over TMZ-treated ($n = 6$; median survival = 30.5 days) or PBS-treated ($n = 7$; median survival = 21 days) mice. *P* values were determined using log-rank test. **d**, GFP and nestin double immunostaining of vestigial tumours in TMZ/GCV-treated *Mut7;Nes-ΔTK* mice (right) versus tumour in control (left) demonstrates depletion of CSCs as evidenced by lack of GFP expression. **e**, Maximal cell density in cortical tumours with different treatment regimens. Untreated *Mut7* mice ($n = 6$) were used as control. Tumour density of 10-week-old non-symptomatic *Mut7* mice (pre-treatment) ($n = 8$) was used as a reference starting point. Cell density was significantly lower in the TMZ/GCV-treated *Mut7;Nes-ΔTK* mice ($n = 6$) compared to untreated tumours ($P = 0.0005$), compared to tumours in pre-treatment mice ($P = 0.004$), and compared to tumours from mice treated with GCV only ($n = 4$). Data are mean ± s.e.m.; $P = 0.001$, Student's *t*-test.

METHODS SUMMARY

Mice. All mice were maintained on a mixed 129SvJ/C57BL/6/B6CAB background. *Mut7* and *Mut7;Nes-ΔTK* mice were obtained by crossing male *hGFAP-Cre;P53$^{fl/fl}$* mice with female *Nf1$^{fl/fl}$;P53$^{fl/fl}$;Pten$^{fl/fl}$;Nes-ΔTK* mice. Genotyping for *Mut7* mice was performed as reported previously[3].

***In vivo* chemical administration.** Stock CldU (Sigma) and BrdU (Sigma) were dissolved in PBS at a concentration of 8.5 mg ml^{-1} and 10 mg ml^{-1}, respectively. 11.5 mg ml^{-1} IdU (MP Biomedicals) solution was made fresh each time[19]. To label dividing cells, 5 ml kg^{-1} stock solution was injected intraperitoneally each time according to the experimental design. GCV (Cytovene-IV, Roche Pharmaceuticals) treatment was performed as described[5]. For initial characterization of *Nes-ΔTK-GFP* mice, 1-month-old *Nes-ΔTK-GFP* or control mice were administered GCV (300 mg kg^{-1} d^{-1}) or PBS via osmotic mini-pump (Model 2002, 0.5 μl h^{-1}, Alzet) for 2 weeks. For treatment starting from 8 or 10 weeks, 150 mg kg^{-1} d^{-1} GCV or PBS was delivered through osmotic mini-pump (Model 2004, 0.25 μl h^{-1}, Alzet); pumps were surgically removed and replaced every 4 weeks based on the experimental requirement. TMZ (Sigma) was dissolved in DMSO and injected intraperitoneally at a dose of 82.5 mg kg^{-1} d^{-1} for 5 days. For the combinational therapy group, mice were first treated with TMZ for 5 days and then osmotic mini-pumps with GCV were implanted 2 days after the last TMZ injection.

Histology and immunohistochemistry. Mice were perfused and brains were processed as described earlier[2]. Paraffin brain haematoxylin and eosin sections (5 μm) were reviewed by J.C. and D.K.B. independently. Tumour type and grades were determined by D.K.B. Fourteen-micrometre cryostat sections were used for GFP/CldU/IdU staining following reported methods[19]. Primary antibodies were

used against GFAP (DAKO, 1:2,000), Olig2 (Millipore, 1:1,000), Sox2 (Millipore, 1:5,000), nestin (BD Biosciences, 1:200), CD44 (BD Biosciences, 1: 75), GFP (Rockland, 1:200, Aves Lab, 1:500), BrdU/IdU (BD Biosciences, 1:100), BrdU/CldU (AbD Serotec,1:500), Ki67 (Novacastra, 1:1,000), PDGFR-α (Santa Cruz, 1:200). Horseradish-peroxidase-based Vectastain ABC Kit (Vector Laboratories) or Cy2/Alexa-488, C3/Alexa555, Cy5-labelled secondary antibodies (Jackson Labs, Invitrogen) were used to visualize the primary antibody staining.

Full Methods and any associated references are available in the online version of the paper.

Received 26 January 2011; accepted 7 June 2012.
Published online 1 August 2012.

1. Chen, J., McKay, R. M. & Parada, L. F. Malignant glioma: lessons from genomics, mouse models, and stem cells. *Cell* **149,** 36–47 (2012).
2. Alcantara Llaguno, S. *et al.* Malignant astrocytomas originate from neural stem/progenitor cells in a somatic tumor suppressor mouse model. *Cancer Cell* **15,** 45–56 (2009).
3. Kwon, C. H. *et al. Pten* haploinsufficiency accelerates formation of high grade astrocytomas. *Cancer Res.* **68,** 3286–3294 (2008).
4. Zhu, Y. *et al.* Early inactivation of p53 tumor suppressor gene cooperating with NF1 loss induces malignant astrocytoma. *Cancer Cell* **8,** 119–130 (2005).
5. Yu, T. S. *et al.* Traumatic brain injury-induced hippocampal neurogenesis requires activation of early nestin-expressing progenitors. *J. Neurosci.* **28,** 12901–12912 (2008).
6. Ishii-Morita, H. *et al.* Mechanism of 'bystander effect' killing in the herpes simplex thymidine kinase gene therapy model of cancer treatment. *Gene Ther.* **4,** 244–251 (1997).
7. Stupp, R. *et al.* Radiotherapy plus concomitant and adjuvant temozolomide for glioblastoma. *N. Engl. J. Med.* **352,** 987–996 (2005).
8. Garcia, A. D. *et al.* GFAP-expressing progenitors are the principal source of constitutive neurogenesis in adult mouse forebrain. *Nature Neurosci.* **7,** 1233–1241 (2004).
9. Deng, W. *et al.* Adult-born hippocampal dentate granule cells undergoing maturation modulate learning and memory in the brain. *J. Neurosci.* **29,** 13532–13542 (2009).
10. Singer, B. H. *et al.* Compensatory network changes in the dentate gyrus restore long-term potentiation following ablation of neurogenesis in young-adult mice. *Proc. Natl Acad. Sci. USA* **108,** 5437–5442 (2011).
11. Snyder, J. S. *et al.* Adult hippocampal neurogenesis buffers stress responses and depressive behaviour. *Nature* **476,** 458–461 (2011).
12. Bao, S. *et al.* Stem cell-like glioma cells promote tumor angiogenesis through vascular endothelial growth factor. *Cancer Res.* **66,** 7843–7848 (2006).
13. Liu, C. *et al.* Mosaic analysis with double markers reveals tumor cell of origin in glioma. *Cell* **146,** 209–221 (2011).
14. Clarke, M. F. *et al.* Cancer stem cells—perspectives on current status and future directions: AACR Workshop on cancer stem cells. *Cancer Res.* **66,** 9339–9344 (2006).
15. Boiko, A. D. *et al.* Human melanoma-initiating cells express neural crest nerve growth factor receptor CD271. *Nature* **466,** 133–137 (2010).
16. Ishizawa, K. *et al.* Tumor-initiating cells are rare in many human tumors. *Cell Stem Cell* **7,** 279–282 (2010).
17. Kelly, P. N. *et al.* Tumor growth need not be driven by rare cancer stem cells. *Science* **317,** 337 (2007).
18. Quintana, E. *et al.* Efficient tumour formation by single human melanoma cells. *Nature* **456,** 593–598 (2008).
19. Vega, C. J. & Peterson, D. A. Stem cell proliferative history in tissue revealed by temporal halogenated thymidine analog discrimination. *Nature Methods* **2,** 167–169 (2005).

Supplementary Information is linked to the online version of the paper at www.nature.com/nature.

Acknowledgements The authors thank S. McKinnon, A. Deshaw, L. McClellan, S. Kennedy and P. Leake for technical assistance, and Parada laboratory members for helpful suggestions and discussion. CldU and IdU preparation and staining protocol was provided by D. A. Peterson at Rosalind Franklin University. This work was supported by grants awarded to S.G.K. (RO1 NS048192-01) and to L.F.P. by the Goldhirsh Foundation, the James S. McDonnell Foundation (JSMF-220020206), Cancer Prevention Research Institute of Texas (RP 100782) and the National Institutes of Health (R01 CA131313). L.F.P. is an American Cancer Society Research Professor.

Author Contributions J.C. and Y.L. performed the experiments. T.-S.Y. and S.G.K. contributed vital reagents. J.C. and L.F.P. designed the experiments. J.C., R.M.M., D.K.B. and L.F.P. analysed the data. J.C., R.M.M. and L.F.P. wrote the paper.

Author Information Reprints and permissions information is available at www.nature.com/reprints. The authors declare no competing financial interests. Readers are welcome to comment on the online version of this article at www.nature.com/nature. Correspondence and requests for materials should be addressed to L.F.P. (luis.parada@utsouthwestern.edu).

METHODS

Mice. All mouse experiments were approved by and performed according to the guidelines of the Institutional Animal Care and Use Committee of the University of Texas Southwestern Medical Center at Dallas. All mice were maintained on a mixed 129SvJ/C57BL/6/B6CAB background. *Mut7* and *Mut7;Nes-ΔTK* mice were obtained by crossing male *hGFAP-Cre;P53*$^{fl/fl}$ mice with female *NF1*$^{fl/fl}$*;P53*$^{fl/fl}$*;Pten*$^{fl/fl}$*;Nes-ΔTK* mice. Genotyping for *Mut7* mice was performed as reported previously[3].

***In vivo* chemical administration.** Stock CldU (Sigma) and BrdU (Sigma) were dissolved in PBS at a concentration of 8.5 mg ml^{-1} and 10 mg ml^{-1}, respectively. 11.5 mg ml^{-1} IdU (MP Biomedicals) solution was made fresh each time[19]. To label dividing cells, 5 ml kg^{-1} stock solution was injected intraperitoneally each time according to the experimental design. GCV (Cytovene-IV, Roche Pharmaceuticals) treatment was performed as described[5]. For initial characterization of *Nes-ΔTK-GFP* mice, 1-month-old *Nes-ΔTK-GFP* or control mice were administered GCV (300 mg kg^{-1} d^{-1}) or PBS via osmotic mini-pump (Model 2002, 0.5 μl h^{-1}, Alzet) for 2 weeks. For treatment starting from 8 or 10 weeks, 150 mg kg^{-1} d^{-1} GCV or PBS was delivered through osmotic mini-pump (Model 2004, 0.25 μl h^{-1}, Alzet); pumps were surgically removed and replaced every 4 weeks based on the experimental requirement. TMZ (Sigma) was dissolved in DMSO and injected intraperitoneally at a dose of 82.5 mg kg^{-1} d^{-1} for 5 days. For the combinational therapy group, mice were first treated with TMZ for 5 days and then osmotic mini-pumps with GCV were implanted 2 days after the last TMZ injection.

Histology and immunohistochemistry. Mice were perfused and brains were processed as described earlier[2]. Paraffin brain haematoxylin and eosin sections (5 μm) were reviewed by J.C. and D.K.B. independently. Tumour type and grades were determined by D.K.B. Fourteen-micrometre cryostat sections were used for GFP/CldU/IdU staining following reported methods[19]. Primary antibodies were used against GFAP (DAKO, 1:2,000), Olig2 (Millipore, 1:1,000), Sox2 (Millipore, 1:5,000), nestin (BD Biosciences, 1:200), CD44 (BD Biosciences, 1: 75), GFP (Rockland, 1:200, Aves Lab, 1:500), BrdU/IdU (BD Biosciences, 1:100), BrdU/CldU (AbD Serotec,1:500), Ki67 (Novacastra, 1:1,000), PDGFR-α (Santa Cruz, 1:200). Horseradish-peroxidase-based Vectastain ABC Kit (Vector Laboratories) or Cy2/Alexa-488, C3/Alexa555, Cy5-labelled secondary antibodies (Jackson Labs, Invitrogen) were used to visualize the primary antibody staining. Images were taken using optical, fluorescence and confocal microscopy (Olympus and Carl Zeiss) and assembled in Adobe Illustrator (Adobe Systems Incorporated).

TMZ, BrdU analogues and pulse-chase experiments. To determine TMZ efficiency, 10- to 11-week-old *Mut7* mice were first injected intraperitoneally with 82.5 mg kg^{-1} d^{-1} TMZ for 5 days. 50 mg kg^{-1} BrdU was injected 2 h after the final TMZ administration and mice were perfused 2 h after BrdU injection. The brain was then paraffin-processed and cut into 5-μm-thick slices. Haematoxylin and eosin staining was performed every 70 μm to identify tumour location. Adjacent tumour sections were selected for GFAP and BrdU co-immunostaining.

For the short-term CldU chase experiments, 10- to 11-week-old *Mut7;Nes-ΔTK* mice were first treated with TMZ for 5 days. A total of three doses of CldU were injected, with 2-h intervals, the day after the final TMZ injection. A single dose of IdU was then injected 3 days after the final TMZ injection. For the long-term CldU chase experiments, 10- to 11-week-old *Mut7;Nes-ΔTK* mice were first treated with TMZ for 5 days. CldU was injected 3 times a day, with 2-h intervals, for 3 days after the final TMZ injection. A single dose of IdU was then injected 7 days after the final TMZ injection. Mice were perfused 2 h after the IdU injection and the brains cryoprotected in 30% sucrose, embedded in OCT, and cut into 14-μm-thick frozen sections. GFAP and Ki67 co-immunostaining was performed every 140 μm to locate the tumour area. Adjacent sections were selected for GFP/CldU/IdU triple immunofluorescence staining.

Quantification. Because of the heterogeneous nature of the tumours, cell density, Ki67 index and BrdU^{+} cell percentage were quantified using the highest staining area[1]. Briefly, staining was checked under low magnification and the highest staining area was identified. The area was viewed at ×200 in three continuous 5-μm-thick sections and positive cells counted using the measured parameters.

For quantification of GFP/CldU/IdU triple staining, tumour areas with at least one CldU^{+} cell were selected, and an 8 μm Z-stack image was scanned and constructed using confocal microscopy (Olympus and Carl Zeiss). A total of ten different areas within each tumour was imaged and subjected to quantification.